Validation of ASTER GDEM over Tibet

By: Simon Billemont, Delft University of Technology

***Abstract*—The Geoscience Lase Altimeter System (GLAS) on board of NASA's ICESat provides a globally distributed dataset, that is well suited for the vertical validation of Digital Elevation Models (DEM's). Recently a new global DEM was created by the Advanced Spaceborne Thermal Emission and Reflection Radiometer (ASTER) on board of NASA's TERRA spacecraft. It provides the so called GDEM with a reported spatial accuracy of about 30m and a vertical accuracy of 20m. Using the GLAS elevation data, these claims can be validated. This article will focus on the validation over the Tibetan plateau. The parameters used for this validation are the local height, slope and roughness.**

The validation procedure revealed a large bias in the data $\pm$30m. Besides this bias, it was shown that the vertical accuracy over flat areas (Nam Co Lake) is very good $\pm$2.8m. However, when the vertical accuracy was computed over a large area, the elevation accuracy decreased to $\pm$11.14m. This is just outside of what is claimed by the release team. Furthermore, a link between the slope/roughness of the terrain was found. For increasing slope/roughness there is also a larger increase in deviation from the ICESat footprints.

***Index Terms*—GDEM, ASTER, ICESAT, TIBET, VALIDATION**

I. Introduction

DIGITAL elevation models (DEM) are widely used in topics related to the state of the terrain in a specific area. Some examples include urban development, hydrological studies, earthquake hazard prediction, etc. [1]. Because of this, there is an increasing demand for more accurate DEMs. In 1999, NASA launched a new spacecraft TERRA [2]. It was the first platform in the Earth Observing System (EOS). On board of TERRA is the ASTER instrument, used for the creation of a new Global DEM (GDEM). This GDEM has a spatial resolution of about 20m. (while Shuttle Radar Topography Mission DEM has a spatial resolution of 90m).

This GDEM was released on June 26, 2009 and is thus relatively new and unverified. The goal in this article is to explain and perform the verification procedure to estimate the accuracy of the ASTER GDEM over the Tibetan plateau. This will be done by comparing the ASTER GDEM with data (height distribution along track) of an another EOS satellite, ICESat [3].

A. Digital elevation model

A digital elevation model (DEM) is a way of digitizing a terrain or elevation map. It is thus a representation of a surface that can be utilized by a computer. One of the currently most used DEMs is the one from the Shuttle Radar Topography Mission (SRTM, 90m spatial resolution). Recently, a new global DEM (GDEM) was released based on observations of ASTER on board of the Terra spacecraft. It has a spacial resolution of 10m (pre-production 20m) vertical and 30m horizontal (95% confidence level [2]). In Figure 1, the ASTER GDEM and SRTM-v3 are shown next to each other.

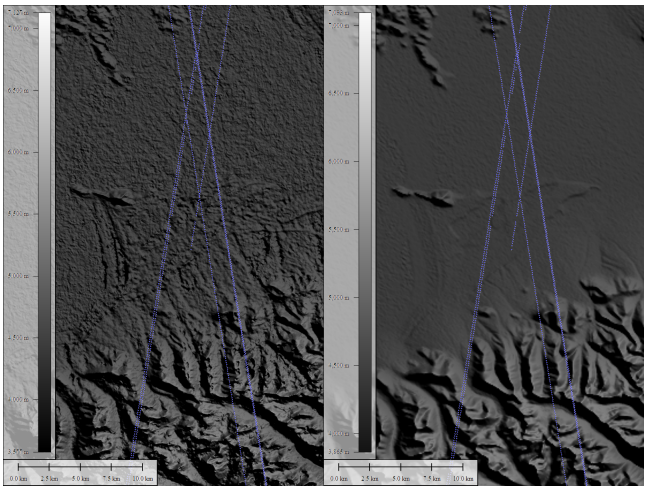

Figure 1. ASTER GDEM (left) and SRTM-v3 (right) comparison with ICESat (L3H-J) tracks over Nam co Lake. Spacial scale bar is 10km.

DEMs are often used for hydrological (e.g. finding water routing over a terrain) and relief studies. For these studies, an accurate DEM is required. This implies that the accuracy of these DEMs needs to be validated. Inaccuracies can be introduced in several ways;

- Inaccuracies in the atmosphere used for the measurement
- Inaccuracies ins the data acquisition equipment
- Inaccuracies and artifacts in the data processing
- Measurement gaps in the data

B. Terra spacecraft

Terra is the flagship of NASA's Earth Observation System (EOS), launched on December 18, 1999. It holds five instruments to observe the earth atmosphere, lands, oceans and radio energy characteristics. The on board instruments have the purpose to better understand the state of the earth and how it is evolving.

NASA has identified several important measurements that would greatly benefit the understanding of the Earth system (atmosphere, land, ocean, ice caps, ...). For a better understanding of this system, NASA developed the Terra spacecraft. Its main goals include [2]:

- providing a global snapshot of Earth surface and atmospheric characteristics (15 years monitoring program);
- improving the ability to detect human impacts on the Earths climate;

Supervisors:
Dr. Roderik Lindenbergh
Lennert van den Berg
Hieu Duong

- improving forecasts of severe climate events;
- improving seasonal and inter annual weather predictions using Terra data;
- begin long-term monitoring of the Earth system to detect changes in global climate and the environment.

To complete this goal, Terra has five instruments to its disposal. Each of these has a specific area of interest. When combining these instruments, a broader understanding of the Earth system can be achieved. The one used to create the GDEM is ASTER (Advanced Spaceborne Thermal Emission and Reflection Radiometer). It is used to create high resolution images of the earth in 14 bands from the visible to the infrared spectrum. ASTER is built up of three instrument subsystems, each with a specific spectral range:

- Visible Near Infrared (VNIR): 0.52-0.86 μm;
- ShortWave Infrared (SWIR): 1.60-2.365 μm;
- Thermal Infrared (TIR): 8.125 - 11.65 μm;

Note these are the ranges of the instruments, not the specific bands. To create the ASTER GDEM, the VNIR sub instrument is used. It has two telescopes, one for nadir looking and one for back looking (along track). The nadir looking telescope has a three-band detector while the back looking telescope only has one-band. The purpose for adding a back looking telescope was to create stereo correlated images in the same band over the same area, from different angles.

When the spacecraft flies over an area, the nadir looking VNIR telescope takes an image of the terrain. About one minute later, the back looking telescope has the same area of land in view and also creates an image (see Figure 2). These two images can then be combined to create a height map using an image stereo correlation algorithm [4].

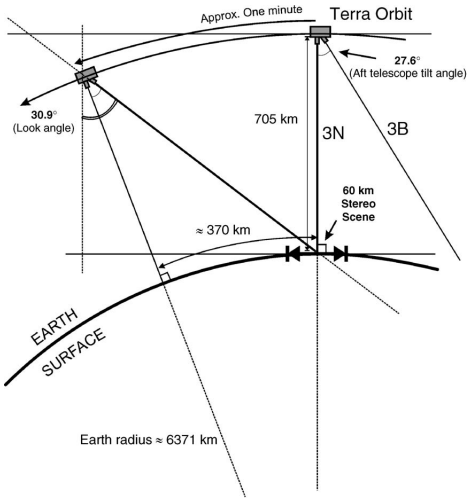

Figure 2. ASTER stereo imaging [5]

This is done by correlating pixels from one image to pixels from the other image. By correlating, one finds pixels in the images that represent the same object. This technique is very accurate for images with lots of variability (contrast). This means that locations where the terrain is uniform, the correlation can give errors, that will propagate into the elevation of that point. When the two equivalent pixels from both images are found, these two pixel locations, with the known locations of the spacecraft and the telescope angles can be combined in a collinearity equation. The collinearity equations are a physical model representing the geometry between a sensor (and its platform), the ground coordinates of an object and the image coordinates. For more information and the exact equations, it is suggested to read [6].

C. ICESat spacecraft

Another satellite in NASA's EOS is ICESat (Ice Cloud and Land Elevation Satellite laser altimeter, launched January 2003). ICESat has one instrument on board, the Geoscience Lase Altimeter System (GLAS). The primary goal of ICESat is to quantify ice sheet mass balance and understand how changes in the Earth's atmosphere and climate affect the polar ice masses and global sea level. ICESat also measured global distributions of clouds and aerosols for studies of their effects on atmospheric processes and global change, as well as land topography, sea ice, and vegetation cover [3]. However on March 29 2003, Laser 1 unexpectedly stopped working after providing about 36 days of data. This was due to a design error in the Laser (present in all the lasers on board). They switched to use Laser 3 for all following measurements until also Laser 3 failed on 19 October 2008. On 11 October 2009, Laser 2 unexpectedly stopped firing. At the time of writing, the GLAS engineering team was investigating the anomaly and evaluating restart plans.

GLAS measures a continuous (during campaigns) track of laser spots. Each spot has a diameter of about 70m and the spots are spaced 172m apart. The instrument works by sending a laser pulse down to earth, and analyzing the returned pulse signal. From the delay between the sent and received pulse, the double distance to the earth can be found by multiplying the delay with the speed of light. The return energy captured as a function of time (the full waveform) of the return signal can provide information about the vegetation, height and cloud distribution (depending on the active laser). These high accuracy laser measurements (~0.15m vertical) can then be used to validate the ASTER GDEM.

The specific ICESat data campaigns used for the validation process are the very first set of campaigns made. The specific campaign numbers are L1A, L2A-1 and L2A-2. The timespan of these campaigns are denoted in Table I.

Table I
ICESAT CAMPAIGN DATES

	Laser 1A	Laser 1B	Laser 2A 8-Day	Laser 2A Pre Delta-T 91-Day	Laser 2A Post Delta-T 91-Day
Start date	20/02/2003	21/03/2003	25/09/2003	4/10/2003	13/10/2003
End date	21/03/2003	29/03/2003	4/10/2003	13/10/2003	19/11/2003

D. Tibetan region

The area for the validation of the ASTER GDEM was chosen to be the Tibetan plateau (Stretching from 30° to 36°N and 85° to 100°E). The Tibetan plateau has extreme fluctuations in both height (2500-6900m) and temperature (-48°C to 35°C) [7], possibly causing large errors in the data. It

holds some of the wold's highest lakes and cities. Furthermore, it has a varied terrain (mountains and plains), vegetation (none to large forest areas) and it contains the sources of the largest rivers in Asia.

To compare the DEM's under different conditions, two study areas were used. The main area chosen is Nam Co Lake (30°42'N 90°33'E). This area was chosen for its very flat terrain. Because of the flatness off this region, it will be used as a baseline for the accuracy of the ASTER GDEM with respect to the ICESat data. Furthermore, a terrain subset (90°-91°E to 31°-37°N) is chosen. In this subset, several ICESat tracks well be used for a statistical analysis. This subset was chosen because it contains a large variety of terrain types.

II. Validation parameters algorithms

A. General validation approach

To compare the DEM's, they first need to be loaded and converted to the same reference system. ASTER GDEM is referenced to the WGS84/EGM96 geoid [8], while ICESat uses the TOPEX/Poseidon ellipsoid as reference. This needs to be converted to the same reference system (WGS84/EGM96). The next step is to compute the characteristics of each DEM so they can be compared. These include local roughness, elevation and slope.

For each data point in the selected study areas, the relevant ICESat footprints are extracted. From this footprint the height is extracted. At the same location, the ASTER GDEM equivalent height is computed. Furthermore the mean slope and roughness are computed. Using this data, a statistical comparison and an estimate for the error can be made. The validation approach is visualized in the flowchart in Figure 3.

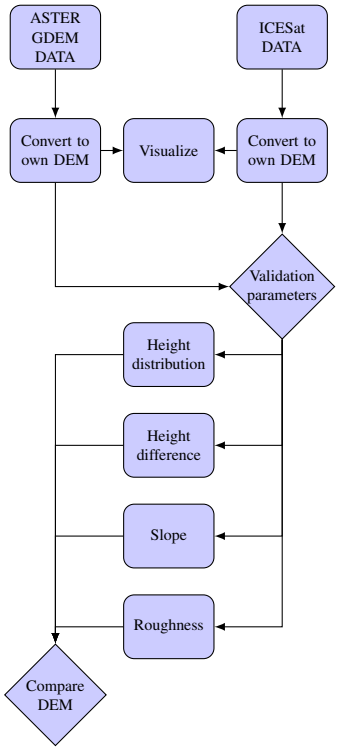

Figure 3. General validation approach

B. Extracting mean height

The elevations of the datapoints in both ASTER and ICESat will be determined relative to the WGS-84 ellipsoid. The ASTER GDEM is already referenced to this ellipsoid. However, since ICESat is referenced to TOPEX/Poseidon, each of the laserspots coordinates needs to be converted into equivalent WGS-84 ones.

The next step is to find the equivalent ASTER height that corresponds with each ICESat data pixel. For this, all the ASTER pixels that overlap with the laserspot are extracted. From these pixels, the weighted average height is extracted and compared with the ICESat data. The weighting is done separately for each ICESat datapoint. The exact method is by creating a mask of pixels (in the ASTER dataset) that are covered by the ICESat footprints. This mask is then normalized and multiplied with the ASTER heights of each pixel. The equivalent height is now the sum of all the values in the mask.

C. Extracting mean slope

Only the mean slope of each relevant data point of the ASTER GDEM is computed. This because ICESat data can only provide the slope in one direction. We know that the slope of a point on the surface $z = f(x, y)$ is given by its gradient at x and y:

$$\varphi = arctan(\sqrt{p^2 + q^2}) \tag{1}$$

With p and q the gradients of the surface (N-S and W-E respectively). To estimate these gradients, a simple although accurate third order Finite Difference (3FD) slope estimation algorithm is used [9].

It works on a local moving 3x3 reference window as depicted in Figure 4. Here g is the spacial resolution of the GDEM, 30m for the ASTER. The 3FD algorithm now estimates p and q from the surrounding points (1-8) using Eq (2) and (3). These two gradients in the two orthogonal directions are then combined to compute the slope in (1).

$$p = \frac{(z_1 - z_6) + (z_2 - z_7) + (z_3 - z_8)}{6g} \tag{2}$$

$$q = \frac{(z_3 - z_1) + (z_5 - z_4) + (z_8 - z_6)}{6g} \tag{3}$$

D. Extracting mean roughness

Roughness of a terrain section, is defined here as the the approximation of actual terrain surface over the projected terrain area (onto the base ellipsoid), see Eq (4) [10]. This gives an estimation of the roughness of a certain area. If the terrain if rough, there is a lot of height variation, causing a large surface area, over a small projected area (roughness is high). If the terrain is smooth, the projected and area surface will be nearly the same, causing a roughness of ≈ 1.

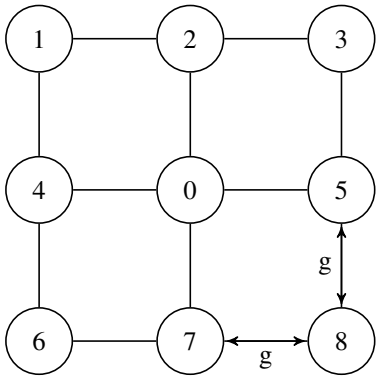

Figure 4. 3x3 moving window

$$R = \frac{S}{A} \tag{4}$$

With R the roughness factor, S the terrain area and A the projected area onto the base plane. The projected area is relatively easy to compute, since it is the spatial resolution squared. On the other hand, to approximate the surface area of the terrain, a more complex algorithm is used.

One starts by defining a new 3x3 moving window. In this window, the center point of each pixel is computed. When these these points are connected, a 3D polygon grid is created, see Figure 5. To approximate the surface of the terrain, we need to compute the surface area of the eight polygons, over the center pixel.

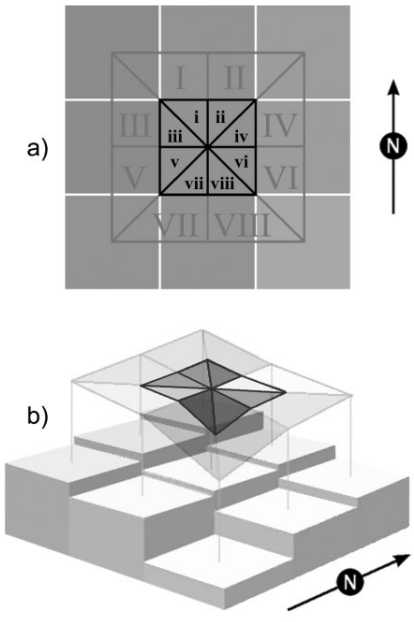

Figure 5. DEM surface approximation. Modified from [10]

The area of each sub-triangle can be found using Eq (5) (from [10]), using the half of the lines connecting the center points. These sub-areas are then summed to form the pixel surface area.

$$S = \sqrt{s(s-a)(s-b)(s-c)} \tag{5}$$

$$\text{with } s = \frac{a+b+c}{2} \tag{6}$$

E. Bias removal

When analyzing the ASTER GDEM, a significant bias with respect to the ICESat data appeared. This bias has to be removed from the ASTER GDEM, so the quality of the ASTER data can be analysed. To remove the bias, the offset (of ASTER) was found where the minimum error existed between the ASTER and ICESat elevations. This was done with a smooth version of both the ASTER GDEM and ICESat footprint tracks. The smoothing technique used a moving average filter with a span of 5. This smoothing was done to prevent local anomalies to affecting the fitting process. This bias removal was done for only one dimension (vertical). The other biases cannot be be removed because the ICESat tracks do not always run parallel to each other.

III. Tools used

For the validation of the ASTER GDEM, several software tools were used. Each of them were used for a specific task.

IDL virtual machine; ITT Visual IDL was used to run provided scripts by the National Snow and Ice Data Center (NSIDC). These scripts converted the ICESat data from binary files to ASCII files which are easier to process. *See http://www.ittvis.com/ProductServices/IDL.aspx* .

MathWorks MATLAB 2008B; MATLAB was used to program the conversion of the ICESat ellipsoid (TOPEX/POSEIDON) to the same ellipsoid as the ASTER data (WGS84). Furthermore, MATLAB was also used to program the comparison algorithms in. This includes matching of ASTER and ICESat data, performing roughness/slope computations and other statistical computations. *See http://www.mathworks.com/* .

Quantum GIS 1.3 was used visualize the ASTER GDEM and to validate the correct matching of ASTER and ICESat data. *See http://www.qgis.org/.*

IV. Validating ASTER GDEM

The most important factor for the validation of the ASTER GDEM is the difference in height with the corrected height of the ICESat laser measurements. On each study area these differences in height will be computed. These can then be combined with the terrain specific features as the mean slope and terrain roughness.

A. Nam Co Lake

The data of three ICESat campaigns were used to validate of the ASTER GDEM (see Figure 6). The ICESat datapoints over Nam Co Lake were extracted and compared to the elevation of the matching data points of the ASTER GDEM over the same lake. The results can be seen in Table II and are visualized in Figure 7. The standard deviation as shown in Table II, was computed using Eq (7).

$$\sigma = \sqrt{\frac{(x_1 - \mu)^2 + (x_2 - \mu)^2 + ... + (x_n - \mu)^2}{N}} \quad (7)$$

Where x_1 to x_n are the values of the heights in each datapoint, μ is the mean height of the entire data sequence and N is the number of datapoints.

Table II
STATISTICS OVER NAM CO LAKE

Campaign	Offset (m)	STD ASTER (m)	STD ICESAT (m)
L1A	-31.7368	2.325466	0.53594
L2A-1	-28.8517	2.337944	2.337944
L2A-2	-32.6986	3.849697	0.135033
Average	-31.0957	2.837702	1.002972

When looking at Figure 7, one notices the large bias in the ASTER data. This bias is estimated to be about -31m (thus the ICESat data is situated 31m under the ASTER data). One explanation for this is that since the ASTER GDEM is constructed from multi-spectral imaging data. This means that the elevation model is constructed at the height of the local vegetation. Nevertheless, this only reason is not enough to explain the type of bias systematically seen in the ASTER elevation with respect to the ICESat elevation. This systematic bias in the data has also been noted in the comparison of the ASTER GDEM with other DEMs:

- $\pm$60 m (mountaineous terrain), $\pm$18 m, (smooth terrain); comparison to a photogrammetric generated DEM [11]
- $\pm$11.6 m compared to USGS 7.5' and SPOT DEMs [12]
- $\pm$7–15 m compared to DGPS and USGS 7.5' DEMs [13]
- $\pm$13 m (RMSE) DGPS [14]
- $\pm$47-96 m compared to TOPO DEM (Andes) [15]

When this bias is removed, the standard deviation of each of the three tracks is about 1.0m for the ICESat footprints. This is most probably due to ice forming over the lake (passes were in the winter, see Table I). For the ASTER data, the standard deviation was 2.8m. This value is well within the region the ASTER GDEM claims to achieve ($\pm$10m vertical).

Due to these winter conditions, ice and snow sheets may form on the lake, causing height differences in elevation with respect to summer conditions. This is only applicable to ICESat data. The reason for this is that the ASTER GDEM was created from observations of the entire lifetime of the satellite.

B. Track L2A-2

To compare the ASTER GDEM over a range of different terrain types, a spatial subset of the L2A-2 campaign was used. This subset is defined by 90°-91°E and 31°-37°N (see Figure 8). From this subset, all the ICESat values and ASTER values are compared using the different statistical tools. Note that the bias has been removed from the dataset. The best fit of the ASTER GDEM to the ICESat footprints was found when the ASTER data was lowered by 32.7m.

The height profile can be found in Figure 9. The jumps in the along track distance are created by switching to another track section and did not effect the outcome of the results. It

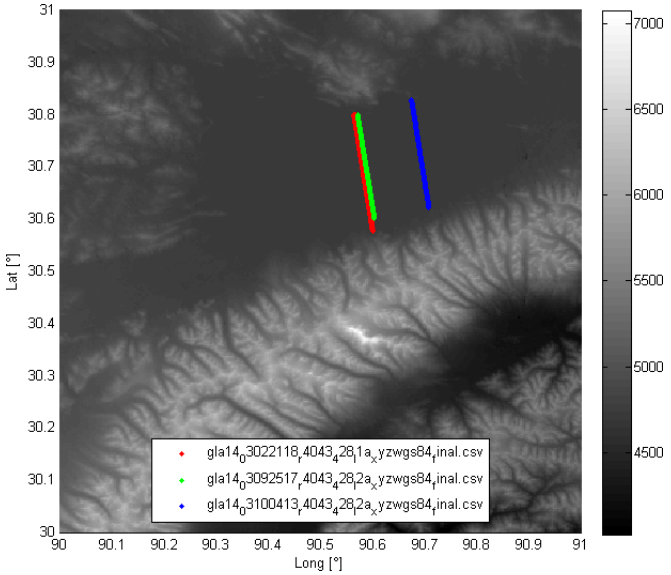

Figure 6. ASTER GDEM and ICESAT tracks over Nam co Lake (elevation in [m])

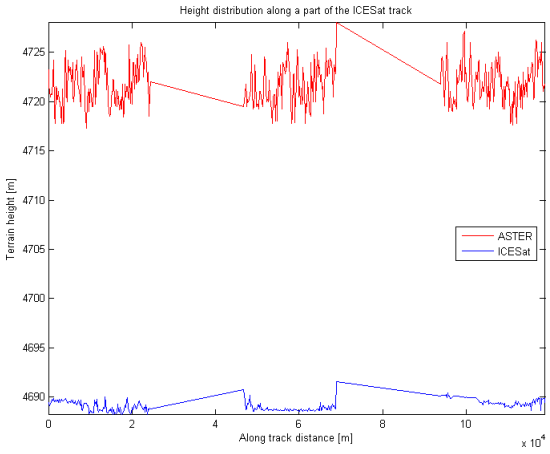

Figure 7. Height distribution along track L1A (with outlier removal)

shows a variety of terrain types including mountains, and a part over Nam Co lake.

In the ASTER GDEM, there were several outliers which where off by more then 500m (see Figure 10). These outliers have been removed by means of discarding everything over 3σ. These outliers are not consistent with the surrounding terrain and are caused by some steep slopes that are missed by the back-looking band or low contrast images (due to snow and ice) [11] [12].

Figure 11 shows that the ASTER GDEM has about the same elevation as the ICESat data. The spread of the ASTER data along these sections is 11.14m. This value is just outside of the bound that where given by the ASTER GDEM specifications. This large value is mostly due to the large terrain variability in the Tibetan region, causing additional errors.

To check if there are relations in the ASTER GDEM elevation errors, a linear approximation to the slope and roughness coefficient were computed. The results are visible in Figure 12-

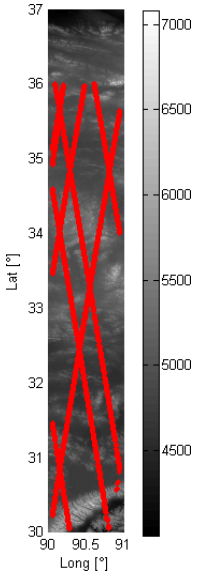

Figure 8. ASTER GDEM and ICESAT tracks (L2A-2) over a subset (no bias, no outliers)

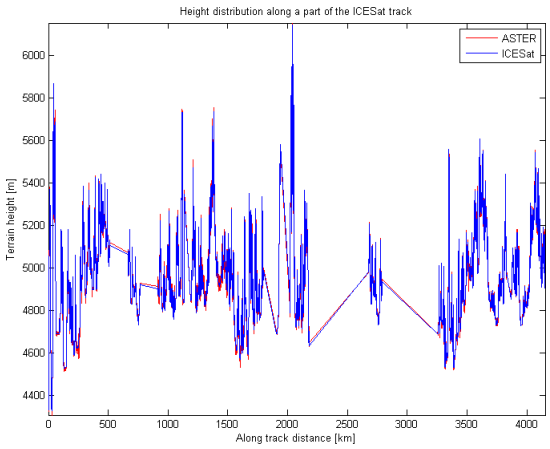

Figure 9. Height distribution along track L2A-2 (removal outliers and bias, elevation in [m])

13. In these figures, the blue dots represent a combination of the slope/roughness of an ASTER datapoint subset, equivalent to an ICESat footprint and the corresponding error. The error is defined as the difference absolute value of ICESat-ASTER. The red line is the first order polynomial that best fits the blue datapoints. Furthermore, the geen bars are the bins of the datapoints.

The roughness coefficient parameter is very sensitive for very rough terrain. Light and medium slopes however do not effect the roughness coefficient a lot. This means that most of the datapoints are in the lower regions of the roughness spectrum. From the scatter plot of the Roughness coefficient (Figure 12), there is a linear trend visible (bins following the red linear approximation closely). This means the increasing roughness coefficient of a certain terrain will lead to larger errors. This is true, even for small changes in the roughness.

The slope of the local terrain is also a good indicator on the terrain geometry. When plotting the relation between the slope

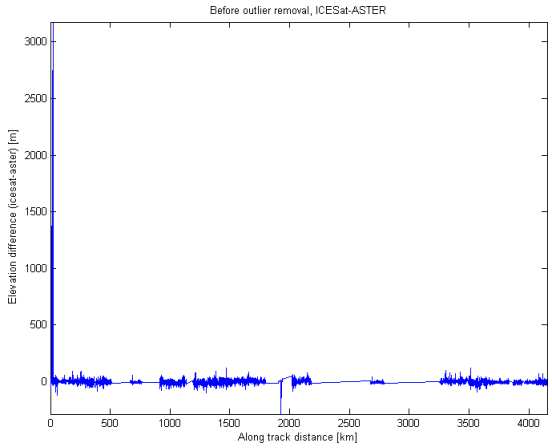

Figure 10. Height distribution along track L2A-2

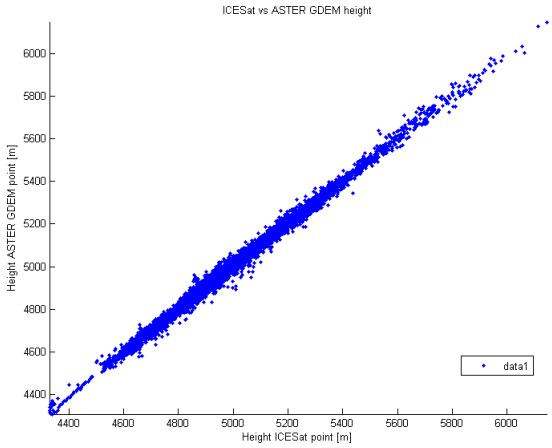

Figure 11. Elevation of ASTER en ICESat compared for L2A-2

and the error in the ASTER GDEM, it is also noticeable that regions with higher slopes are more prone to larger errors. This is especially true for regions with a slope in excess of 60°. In those regions, there is a large increase in error. This can mainly be attributed to the overlooking of certain faces by the back looking telescope. For the smaller slopes the relationship the error has with the slope is comparable with what was found when comparing the roughness of the terrain.

Some of these errors are introduced by artifacts from the automated GDEM creation algorithm used. This algorithm uses all high quality images for a certain region. Since the number of these images varies per region, anomalies appear on the boundaries of two such regions. These anomalies cause artificial height variation, and can be filtered out using appropriate algorithms. Due to the scope and limited time in this project, it was chosen not to do this.

V. Conclusions and Recommendations

Digital elevation models are widely used these days for a wide range of applications. For most applications, accurate DEMs are required. For this reason, the DEMs claims on accuracy need to be validated. The ASTER GDEM, released June 29th 2009, claims it can achieve a vertical accuracy of 10m.

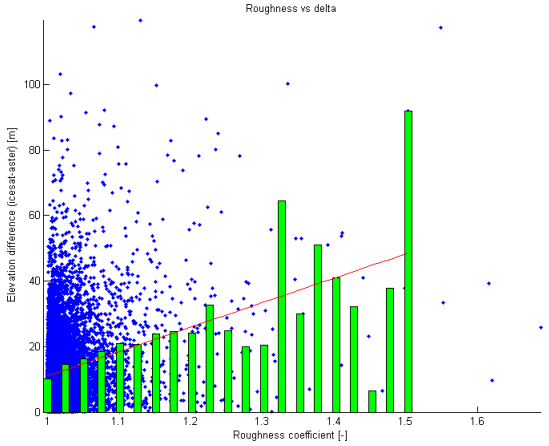

Figure 12. Roughness coefficient vs elevation difference (bins at 40% width)

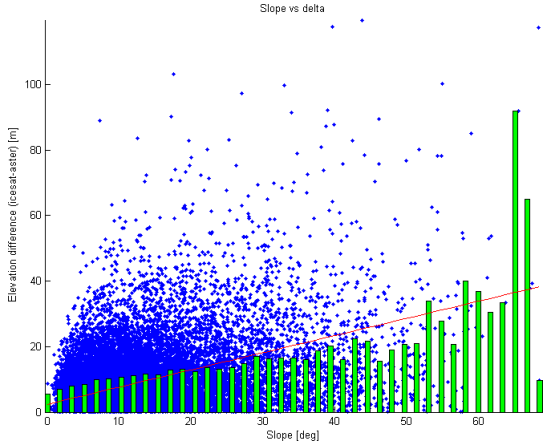

Figure 13. Slope vs elevation difference (bins at 40% width)

This accuracy was tested with respect to three campaign of the ICESat altimeter (L1A/L2A-1/L2A-2). For the validation two specific regions were used. These are Nam Co Lake and an subset in Tibet.

Over Nam Co Lake, this level of vertical accuracy was reached with an average deviation of $\pm$2.8m. However, in the ASTER GDEM, there is a large bias. This bias is -31m (thus 31m above the ICESat footprints).

The other site investigated is a subset over Tibet reaching from 90°-91°E to 31°-37°N. In this region also a bias in the data was found (-32.7m). Besides this bias, there where several peaks in the data. These peaks are very high above the rest of the ASTER GDEM surface and are therefor easily filtered out. The standard deviation over this subset was found to be 11.14m with respect to the ICESat data. This value is slightly higher that what is claimed the GDEM can achieve, but this is of course the most extreme type of terrain available. Furthermore it was investigated if there was a relationship in the vertical elevation error with the slope of the terrain and the the terrain roughness. A relation was found for both the roughness and the slope. For increasing slope/roughness there was also a systematic increase in error.

The ASTER GDEM does not appear to be everywhere under the vertical accuracy of 10m. It must be noted however that it does meet the pre-production estimated vertical accuracy of 20m. Some areas have a higher accuracy and some a lower one then the 10m vertical. This is mainly due to terrain geometry and pointing errors.

The recommendation on the validation of the ASTER GDEM is to try filtering out artifacts that have been introduced in the automated ASTER GDEM creation. These include residual cloud anomalies and anomalies that appear do to the different stacking of images used to create the DEM. Also using an estimate of the ice and snow coverage in the reference elevations (ICESat in this case) could be used to validate the ASTER GDEM more accurately.

A digital version of this document is also available at *http://permanent.angelcorp.be/ASTER*.

REFERENCES

[1] A. R. Darnell, N. J. Tate, and C. Brunsdon, "Improving user assessment of error implications in digital elevation models," *Computers, Environment and Urban Systems*, vol. 32, no. 4, pp. 268 – 277, 2008, geographical Information Science Research - United Kingdom. [Online]. Available: http://www.sciencedirect.com/science/article/B6V9K-4SDNK3H-1/2/a6b1482f7af589da0c1a9743574fad60

[2] (2009, September) The terra spacecraft. NASA. Goddard Space Flight Center. [Online]. Available: http://terra.nasa.gov/About/

[3] (2009, September) Icesat home page. NASA. Goddard Space Flight Center. [Online]. Available: http://icesat.gsfc.nasa.gov/

[4] H. R. Arabnia, "Distributed stereo-correlation algorithm," *Computer Communications*, vol. 19, no. 8, pp. 707 – 711, 1996, selected papers from the Third International Conference on Computer Communications and Networks. [Online]. Available: http://www.sciencedirect.com/science/article/B6TYP-3VV6NFN-14/2/b0284e08e8bd9dc69e000e86fb812275

[5] A. Hirano, R. Welch, and H. Lang, "Estimating vertical error of srtm and map-based dems using icesat altimetry data in tibetan plateau," *ISPRS Journal of Photogrammetry and Remote Sensing*, vol. 57, no. 5-6, pp. 356 – 370, 2003, challenges in Geospatial Analysis and Visualization. [Online]. Available: http://www.sciencedirect.com/science/article/B6VF4-47VH5SJ-3/2/813f883c265218f3585fc7b3f2bffa22

[6] X. Ping, "Digital elevation model extraction from aster in support of the coal fire and environmental research project china," Ph.D. dissertation, ITC. pp 1-92, 2003.

[7] X. Huang, H. Xie, T. Liang, and D. Yi, "Accuracy estimation of strm and map-based dems using icesat elevation in tibetan plateau," 2009.

[8] *ASTER GDEM Readme File – ASTER GDEM Version 1*, na Std., 2009. [Online]. Available: http://www.ersdac.or.jp/GDEM/E/image/ASTER\%20GDEM\%20Readme_Ev1.0.pdf

[9] Q. Zhou, B. Lees, and G. an Tang, *Advances in Digital Terrain Analysis*. Springer Berlin Heidelberg, 2008, ch. Accuracy Assessment of DEM Slope Algorithms Related to Spatial Autocorrelation of DEM Errors, pp. 307–322, section 4.

[10] J. S. Jenness, "Calculating landscape surface area from digital elevation models," *Wildlife Society Bulletin*, vol. 32, no. 3, pp. 829–839, Sep. 2004. [Online]. Available: http://dx.doi.org/10.2193/0091-7648(2004)032[0829:CLSAFD]2.0.CO;2

[11] A. Kääb, C. Huggel, F. Paul, R. Wessels, B. Raup, H. Kieffer, and J. Kargel, "Glacier monitoring from aster imagery: accuracy and applications," in *Proceedings of EARSeL LIS-SIG Workshop*, 2002, march 11–13.

[12] T. Toutin and P. Cheng, "Comparison of automated digital elevation model extraction results using along-track aster and across-track spot stereo images," *Optical Engineering*, vol. 41, no. 9, pp. 2102–2106, 2002. [Online]. Available: http://link.aip.org/link/?JOE/41/2102/1

[13] A. Hirano, R. Welch, and H. Lang, "Mapping from aster stereo image data: Dem validation and accuracy assessment," *ISPRS Journal of Photogrammetry and Remote Sensing*, vol. 57, pp. 356–370(15), April 2003. [Online]. Available: http://www.ingentaconnect.com/content/els/09242716/2003/00000057/00000005/art00164

[14] A. Cuartero, A. Felicisimo, and F. Ariza, "Accuracy, reliability, and depuration of spot hrv and terra aster digital elevation models," *IEEE Transactions on Geoscience and Remote Sensing*, vol. 43, no. 2, pp. 404–407, February 2005.

[15] A. E. Racoviteanu, W. F. Manley, Y. Arnaud, and M. W. Williams, "Evaluating digital elevation models for glaciologic applications: An example from nevado coropuna, peruvian andes," *Global and Planetary Change*, vol. 59, no. 1-4, pp. 110 – 125, 2007, mass Balance of Andean Glaciers. [Online]. Available: http://www.sciencedirect.com/science/article/B6VF0-4MSR8S6-3/2/8a020508ea1b14f6bfe4848d601eb1c0

[16] A. Bolten and O. Bubenzer, "New elevation data (srtm/aster) for geomorphological and geoarchaeological research in arid regions," *Zeitschrift für Geomorphologie / Supplement*, vol. 142, pp. 265–279, 2006.

[17] C. Carabajal and D. Harding, "Srtm c-band and icesat laser altimetry elevation comparisons as a function of tree cover and relief," *Photogrammetric Engineering & Remote Sensing*, vol. 72, no. 3, pp. 287–298, March 2006.

[18] C. C. Carabajal and D. J. Harding, "Icesat validation of srtm c-band digital elevation models," *GEOPHYSICAL RESEARCH LETTERS*, vol. 32, October 2005, l22S01.

[19] ——, "Icesat waveform measurements of within-footprint topographic relief and vegetation vertical structure," *GEOPHYSICAL RESEARCH LETTERS*, vol. 32, October 2005, l21S10.

[20] C. G. DE OLIVEIRA and W. R. PARADELLA, "Evaluating the quality of the digital elevation models produced from aster stereoscopy for topographic mapping in the brazilian amazon region," *Anais da Academia Brasileira de Ciencias ISSN 0001-3765 CODEN AABCAD*, vol. 81, pp. 217–225, 2009.

[21] S. Hook, Arai-San, K. Thome, H. Kieffer, R. Alley, P. Palluconi, A. Gillespie, R. Feind, and H. Lang, "Aster validation plan," NASA, 1999. [Online]. Available: http://hdl.handle.net/2014/18839

[22] METTI/ERSDAC, NASA/LPDAAC, and USGS/EROS, "Aster glabal dem validation, summary report," June 2006.

[23] S. Mitchell, *Geoscience Laser Altimeter System: Validation of Altimetry and Atmospheric Backscatter Data*, University of Colorado at Boulder Std., April 2009.

[24] B. E. Schutz, "Spaceborne laser altimetry: 2001 and beyond," 1998, published in Plag, H.P. (ed.), Book of Extended Abstracts, WEGENER-98, Norwegian Mapping Authority, Honefoss, Norway.

[25] S. D. Warren, M. G. Hohmann, K. Auerswald, and H. Mitasova, "An evaluation of methods to determine slope using digital elevation data," *CATENA*, vol. 58, no. 3, pp. 215–233, December 2004. [Online]. Available: http://dx.doi.org/10.1016/j.catena.2004.05.001

[26] (2009, September) Asterweb. NASA. Goddard Space Flight Center. [Online]. Available: http://asterweb.jpl.nasa.gov/